ELSEVIER

International Journal of Mass Spectrometry 205 (2001) 183–196

International Journal of Mass Spectrometry

VUV optical absorption and energy loss spectroscopy of chlorine nitrate

N.J. Mason[a,*], N.C. Jones[a], L. Kaminski[a], B.A. Osborne[b], G. Marston[b], M.A. Fernandez[b], I.C. Walker[c], E.A. Seddon[d], J. Ballard[e], and D.A. Newnham[e]

[a]*Department of Physics and Astronomy, University College London, Gower Street, London, WC1E 6BT, England*
[b]*Department of Chemistry, University of Reading, Whiteknights, P.O. Box 224 Reading, RG6 6AD, England*
[c]*Department of Chemistry, Heriot-Watt University, Riccarton, Edinburgh, EH14 4AS, Scotland*
[d]*CLRC Daresbury Laboratory, Daresbury, Warrington, Manchester, WA4 4AD, England*
[e]*Molecular Spectroscopy Facility, Space Science Department, Rutherford Appleton Laboratory, Chilton, Didcot, Oxon OX11 0QX, England*

Received 24 July 2000; accepted 4 August 2000

Abstract

The electronic spectroscopy of the stratospheric compound chlorine nitrate ($ClONO_2$) has been probed using photoabsorption, photoelectron, and electron energy loss spectroscopy. Spectral assignments for the observed features are discussed. (Int J Mass Spectrom 205 (2001) 183–196) © 2001 Elsevier Science B.V.

Keywords: VUV; Ozone depletion

1. Introduction

Stratospheric ozone depletion is a serious problem, both globally [1] and, more dramatically, during the Antarctic [2] spring; ozone depletion during the Arctic spring is also becoming increasingly common [3]. There is convincing evidence that much ozone depletion occurs as a direct consequence of the anthropogenic emission of chlorine-containing compounds into the atmosphere [4]. As a result of the Montreal Protocol [5], emissions of chlorofluorocarbons (CFCs) have been drastically reduced, and there is now evidence to suggest that their atmospheric concentrations are dropping, at least in the lower atmosphere [6,7]. Nevertheless, ozone depletion at the poles is expected to continue and, indeed, get worse in coming years because the stratosphere is cooling, possibly because of increased emissions of greenhouse gases, which act as icehouse gases in the stratosphere [8]. Low temperatures are a key ingredient in polar ozone depletion [9], allowing the formation of polar stratospheric clouds (PSCs), which catalyze the conversion of reservoir compounds into photolabile species that readily release atomic chlorine. One such reaction is

$$ClONO_2 + HCl \rightarrow HNO_3 + Cl_2. \quad (1)$$

In this process, the HNO_3 becomes part of the cloud particle, while Cl_2 is released to the gas phase, where

* Corresponding author. E-mail: nigel.mason@ucl.ac.uk

Dedicated to Professor Aleksandar Stamatovic on the occasion of his 60th birthday.

PII S1387-3806(00)00375-4

it is rapidly photolyzed when the sun illuminates the atmosphere in the polar spring. Chlorine nitrate, $ClONO_2$, is, under normal circumstances, an effective reservoir for the active ClO_x and NO_x species; it is formed by the reaction

$$ClO + NO_2 + M \rightarrow ClONO_2 + M \quad (2)$$

and is subsequently photolyzed on a timescale of several hours to produce a mixture of NO_x and ClO_x products [10]. Since the importance of chlorine nitrate in determining stratospheric ozone concentrations was recognized, there have been a number of studies of its structure, spectroscopy, and photochemistry. Rowland et al. [11] measured its UV spectrum at room temperature between 186 and 460 nm. The temperature dependence of the UV absorption cross sections has been determined by Molina and Molina [12] and Burkholder et al. [13] with good agreement between the two groups. Recent studies of the photochemistry of chlorine nitrate are summarized in evaluation 12 of the NASA Panel for Data Evaluation [10]. The channel leading to $Cl + NO_3$ appears to dominate, although the $ClO + NO_2$ is significant at least at wavelengths $<$350 nm (3.75 eV). Nikolaisen et al. [14] have observed a strong pressure dependence in the dissociative channel, particularly at wavelengths $>$330 nm. A single theoretical study of the excited electronic states of chlorine nitrate has been reported [15], and we will refer to this in making spectral assignments here.

The photoelectron spectrum (PES) of $ClONO_2$ has also been published recently [16], and peaks were assigned using the results of ab initio calculations [17]. The chlorine nitrate anion, $ClONO_2^-$ has been prepared by charge transfer processes; from these, it has been deduced that the electron affinity (EA) lies between 2.1 and 3.1 eV. The calculated adiabatic EA is 2.9 eV ± 10%, while the vertical detachment energy is estimated at 4.49 eV [18,19]. Like the neutral molecule, the anion is planar; extra electron density is concentrated around the N atom, and the Cl–O bond is elongated so that the species looks like $Cl–NO_3^-$. The cross section for attachment of free thermal electrons to $ClONO_2$ is very large, but the anion dissociates, major product ions being NO_2^- (∼50%), NO^- (30%), and ClO^- (∼20%) [18,19].

In this article, we augment the earlier work by presenting electronic excitation spectra of chlorine nitrate obtained using both optical absorption (VUV) and electron energy loss (EEL) techniques. Employing these methods, we have extended the spectral range to ∼80 nm (15 eV), allowing some spectral features to be observed for the first time. We have also recorded a photoelectron spectrum for comparison with earlier data. Measurements using near-threshold EEL spectroscopy are also reported, providing information on both low-lying triplet excited states (which may be implicated in its photochemistry) and $ClONO_2^-$ anionic states. This work is part of an ongoing program on the spectroscopy of molecular species pertinent to stratospheric ozone depletion (e.g., O_3 [20], Cl_2O [21], OClO [22], and N_2O_5 [23]).

2. Experimental methods

2.1. Production of samples of chlorine nitrate

Chlorine nitrate was prepared by allowing a mixture of Cl_2O and N_2O_5 to warm up overnight from 195 K to ∼273 K [24]. The resultant product mixture (mainly Cl_2 and $ClONO_2$) was a strong, clear, yellow color. Purification by trap to trap distillation removed residual molecular chlorine to yield $>$90% of the chlorine nitrate in the form of a pale yellow/green liquid. N_2O_5 was synthesized from the reaction of NO with ozone [23]. Cl_2O was generated by passing molecular chlorine over dry mercuric oxide [21]. The purity of the chlorine nitrate samples was monitored by measuring the photoabsorption cross section at 240 nm using a standard laboratory spectrophotometer (Kontron Uvikon 860). The derived cross section (1.04×10^{-18} cm^2) matches the recommended NASA value of 1.04×10^{-18} cm^2.

2.2. Photoabsorption spectra

Photoabsorption spectra were measured between 300 and 140 nm (5–8.8 eV) using synchrotron radi-

ation derived from the UK Daresbury facility. For these experiments, an absorption cell was capped with LiF windows and the sample was flowed continuously through the cell. Transmitted radiation was detected using a sodium salicyclate quantum converter and photomultiplier tube. The absorption path length was 16 cm, and spectra were recorded at step lengths of 0.1–0.5 nm. Pressures were measured using a Baratron capacitance manometer. Radiation transmitted in the presence of sample (I_t) was recorded at each wavelength along with sample pressure and decreasing synchrotron ring current. The sample flow was then stopped and radiation intensity through the empty cell (I_0) measured along with ring current at the same selected wavelengths. Digitized data were stored and radiation intensities normalized to a constant ring current before analysis using the Beer-Lambert expression

$$I = I_0 \exp(-n\sigma x), \quad (3)$$

where σ is the absorption cross section, n the gas number density, and x the path length. Further details on the apparatus are given in earlier publications [20–23].

Additional experiments were carried out using a conventional UV-Vis spectrometer (Kontron Uvikon 860) at the University of Reading and a Bruker IFS 120HR Fourier transform spectrometer modified for use down to wavelengths as short as 260 nm. (This instrument is based at the Molecular Spectroscopy Facility at the Rutherford Appleton Laboratory [RAL].) The details of these modifications are given elsewhere [23], but a brief description is given here. The optical configuration of the spectrometer was changed to reduce losses caused by reflections, and an aluminium-coated quartz beam-splitter was put in place. The light source was a quartz-tungsten-halogen lamp (Philips type 7158), and a solar-blind UV photodiode was used as the detector. The spectrometer was operated at a resolution of 4 cm^{-1} ($\approx$0.025 nm at the wavelengths used). Both the Reading and RAL measurements were made using borosilicate glass cells with quartz windows. Absorption measurements were made with static samples in the cell, and background spectra were recorded with the cell evacuated.

2.3. Electron energy-loss spectra

The high-energy electron energy-loss spectrometer (EELS) employed an electron beam of energy 150 eV crossing a molecular beam of the target gas with energy analysis and collection of electrons scattered through small angles centered around 0° [25]. Inelastic electron-molecule scattering experiments performed using this kind of instrument may be used to determine photoabsorption cross sections as long as certain conditions are fulfilled. At high-incident electron energies, electron scattering may be described using the first Born approximation through which the generalized oscillator strength (GOS) was introduced [26]. Specifically, the GOS connects the cross sections derived from optical studies with those obtained from electron scattering in the limit of zero-momentum transfer [27]. The necessary conditions are met experimentally when the kinetic energy of the incident electrons (T) is sufficiently high, the energy transferred to the target (E) is moderate ($E/T < \sim 10\%$), and the scattering angle is small ($\theta_s \sim 0°$). Then, raw data from an electron-scattering experiment may be converted into relative differential oscillator strengths using the method of Huebner et al. [27]; these relative values may be put on an absolute scale by normalizing to a known photoabsorption cross section at an energy at which the cross section does not vary rapidly with energy.

To ensure that the above conditions are met, it is common to use incident electron beams having 3 keV (or higher) incident energy and scattering angles centered on 0° [28,29]. However, in practice it has been found that electron energies an order of magnitude smaller can be used [30]. Indeed, electron energies as low as 100 eV have been employed routinely to obtain reliable oscillator strengths for a range of molecules; for example, molecular oxygen [31], acetone [27], naphthalene [32], and several monosubstituted benzene derivatives [33]. We have used the analysis algorithm derived by Huebner et al. [27] to convert EEL spectra obtained on the present instrument (T = 150 eV, $\theta_s \sim 0°$) to oscillator strengths for a number of molecules, including ozone [34], chlorine dioxide [35], formamide [36], benzyl alcohol

[37], and several alkanes and alkenes [38,39]. In all cases, the transformed data agreed well with measured optical spectra and also, for the hydrocarbons, with EEL spectra recorded using 3 keV electrons. We have therefore used this method to relate high-energy ($T = 150$ eV) data for chlorine nitrate to the optical absorption spectra. The high-energy EEL spectrum was normalized to the VUV cross sections at 230 nm (5.4 eV).

2.4. The trapped electron spectrometer and anion detection

Low-energy electron impact data were obtained using a trapped-electron spectrometer in which the energy of the incident electrons (moving under the influence of an axial magnetic field) is selected in a trochoidal electron mono-chromator [40,41]. The sample was flowed through the collision region mixed with helium. The electrode potentials in the collision region are such that any inelastically scattered electrons whose energy is between 0 and a preset value W eV are trapped and collected on a surrounding cylindrical collector. The resulting spectrum is a near-threshold electron energy-loss spectrum at a residual electron energy of W. In this mode, the electron energy-loss axis was calibrated from the helium 2^3S transition at 19.81 eV. As well as low-energy electrons, negative ions formed in resonant dissociative electron attachment are also trapped in the interaction region; these can be identified independent of the electrons because they persist at zero well depth, when electrons are no longer trapped. Under these conditions, the energy axis was calibrated by assuming that the lowest DEA energy is at 0 eV [18,19]. Signal arising from scattered electrons was obtained by subtraction of the negative ion signal from a composite spectrum.

2.5. The photoelectron spectrometer

Photoelectron spectra were recorded using an angle-resolving UV photoelectron spectrometer built in-house at Daresbury Laboratory. A commercial (Vacuum Generators) helium lamp was used to provide incident 58.43 nm (21.2 eV) radiation. The photoelectrons were energy analyzed in a hemispherical electron monochromator fitted with channel plates and a resistive anode encoder at its exit aperture [42]. The energy scale of the photoelectron spectrum was calibrated using the well-known photoelectron spectrum of molecular nitrogen.

3. Results

3.1. Photoabsorption spectra

The VUV photoabsorption spectrum of $ClONO_2$ in the range 4.1–9.0 eV is presented in Fig. 1a. Below 6.2 eV, the spectrum shows a broad featureless continuum centered around 5.77 eV with a minimum at 6.0 eV and a steady increase in cross section above the minimum. These observations are in broad agreement with those reported by Burkholder et al. [13], who used a laboratory UV-Vis spectrometer (these data form the basis of the NASA recommendation). The cross sections above 210 nm determined using the conventional spectrometer and the Fourier transform spectrometer are compared with the synchrotron data in Fig. 1b. There are some differences, which are considered in the Discussion. Apart from the work of Rowland et al., [11] who obtained data at energies up to 6.8 eV, the present investigation sees the photoabsorption spectrum above 6.2 eV for the first time. Between 6.2 and 9.0 eV, there is a second broad band, centered at 8.0 eV, with a shoulder on its rising side around 7.1 eV. After a minimum at ~8.65 eV, the cross section begins to rise again; this rise is confirmed by the energy-loss spectra reported below. As an additional check on the cross sections obtained from the Daresbury data, $\ln(I_0/I_t)$ ($= n\sigma x$, where n is gas number density, σ is the cross section, and x the path length) was obtained as a function of gas pressure at three fixed wavelengths, and each cross section was evaluated from the resulting linear plot. These cross sections (Fig. 1a) agree with the fixed pressure measurements, confirming that the latter were made at sufficiently low pressures to ensure the absence of saturation effects.

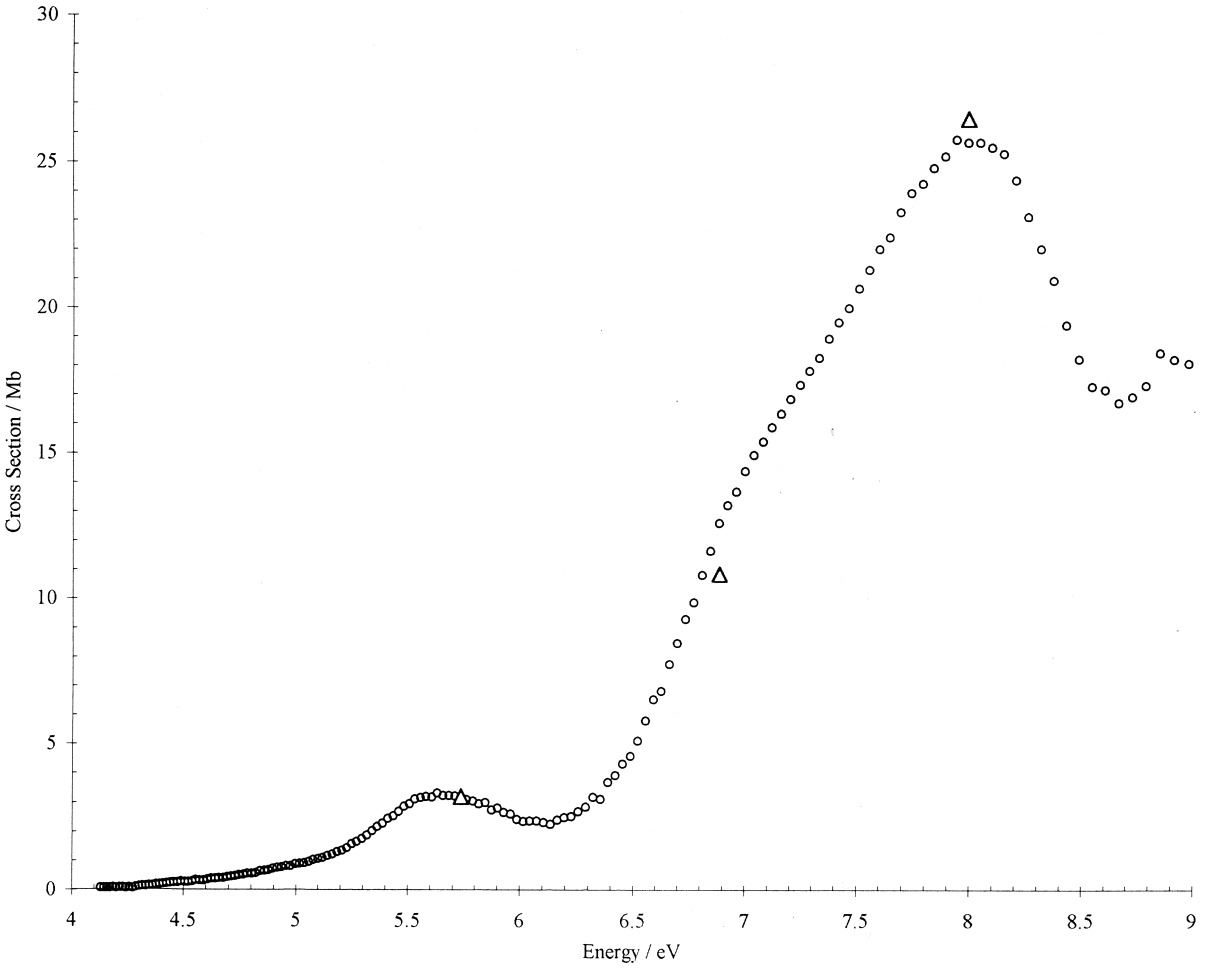

Fig. 1. (*a*) VUV photoabsorption spectra of chlorine nitrate between 240 and 120 nm recorded using synchrotron radiation at the UK Daresbury facility. (*b*) UV photoabsorptoin spectra of chlorine nitrate obtained using a variety of techniques.

3.2. Electron energy-loss spectra

The differential oscillator strength (DOS) spectrum derived from the high–incident energy EEL data is shown in Fig. 2, and the cross sections are listed in Table 1. The DOS spectrum was normalized at an energy of 5.4 eV to the results of Burkholder et al. [13]. The DOS and photoabsorption data (Fig. 3) agree within the combined error limits (see below). Above the high-energy cut-off of the photoabsorption spectrum, the EEL spectrum shows a strong maximum at 9.26 eV, with other features at 9.38, 9.74, 10.66, 10.93, 11.47, and 12.98 eV.

3.3. Trapped electron spectra

The total negative ion signal following dissociative electron attachment (DEA) to $ClONO_2$ is shown in Fig. 4a, and a scattered electron spectrum at an residual electron energy of ~0.5 eV is shown in Fig. 4b. The present low-energy impact data confirm earlier observations [18,19] that the cross section for formation of negative ions is very large at energies close to 0 eV; we assumed the energy of maximum cross section to be zero. The cross section for DEA has maxima at ~0, 3.0, and 5.7 eV, respectively. Cross sections for inelastic excitation have maxima of

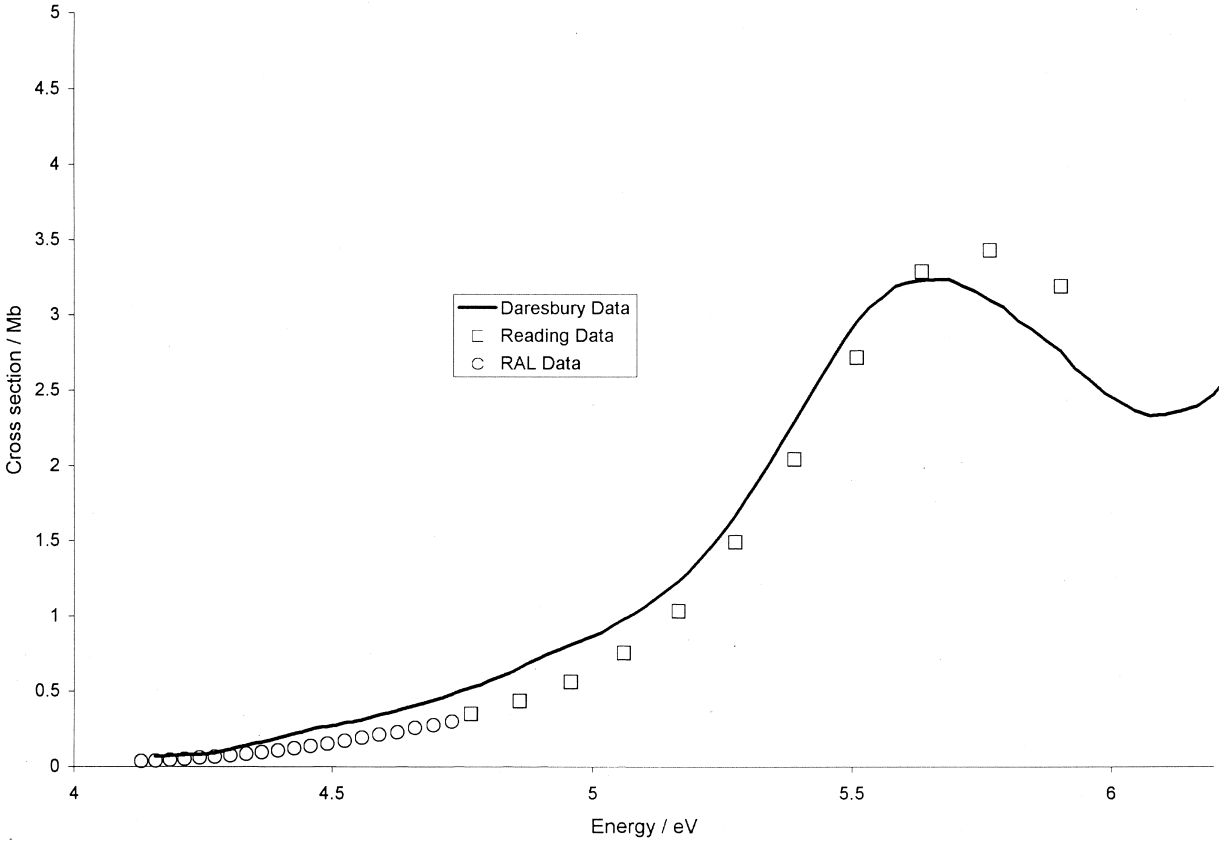

Fig. 1b. Differential oscillator strength spectrum for chlorine nitrate derived from electron energy-loss spectrum recorded using the UCL EELS.

~3.2, 6.0, 7.0, and 8.0 eV. The first energy-loss process spans the two lowest absorption bands in the UV spectrum [13], with the maximum matching that of the first optical band (3.2 eV). Otherwise, the electron impact behavior confirms the presence of several electronic states between ~5 and 9 eV.

3.4. Photoelectron spectra

From previous work [16], the principal electron configuration of $ClONO_2$ (a planar molecule of C_s symmetry)

$$(3a'')^2(17a')^2(18a')^2(4a'')^2(19a')^2(5a'')^2.$$

Our photoelectron spectrum (Fig. 5) is consistent with the only other reported spectrum [16], but it is marginally less well resolved. In the earlier work, bands 1–3 showed weak vibrational structure, which is not visible in the present data. These three bands have been ascribed to removal of electrons (in order of increasing ionization energy) from orbitals 5a″ (π type, localized on the NO_2 end), 19a′ (σ, nCl), and 4a″ (π); together with 18a′(σ), the last two ionizations were contained within band 3. Higher-lying bands are broad and structureless and so have been attributed to ionization of strongly bonding electrons [16].

4. Discussion

4.1. Absolute photoexcitation cross sections

The data plotted in Fig. 1b show that, at long wavelengths, the cross sections obtained at Daresbury

Table 1a
Photoabsorption cross sections for chlorine nitrate recorded using laboratory UV-Vis spectrometer at Reading University ($210 < \lambda < 260$) and Fourier Transform spectrometer at Rutherford Appleton Laboratory ($265 < \lambda < 300$)

λ/nm	Energy/eV	VUV xsn/Mb
210	5.90	3.18
215	5.76	3.42
220	5.63	3.28
225	5.51	2.71
230	5.39	2.04
235	5.27	1.49
240	5.17	1.03
245	5.06	0.75
250	4.96	0.56
255	4.86	0.43
260	4.77	0.35
265	4.68	0.26
270	4.59	0.21
275	4.51	0.16
280	4.43	0.11
285	4.35	0.08
290	4.27	0.06
295	4.20	0.04
300	4.13	0.03

Table 1b
Photoabsorption cross sections for chlorine nitrate derived from synchrotron measurement

λ/nm	Energy/eV	VUV xsn/Mb
140	8.85	18.43
145	8.55	17.27
150	8.26	23.11
155	8.00	25.66
160	7.75	23.93
165	7.51	20.65
170	7.29	17.82
175	7.08	15.40
180	6.89	12.53
185	6.70	8.46
190	6.52	5.10
195	6.36	3.11
200	6.20	2.48
205	6.05	2.37
210	5.90	2.81
215	5.76	3.09
220	5.63	3.32
225	5.51	2.94
230	5.39	2.28
235	5.27	1.66
240	5.16	1.22
245	5.06	0.96
250	4.96	0.81
255	4.86	0.65
260	4.77	0.53
265	4.68	0.41
270	4.59	0.33
275	4.51	0.27
280	4.43	0.22
285	4.35	0.15
290	4.27	0.08
295	4.20	0.07
300	4.13	0.07

are higher than the other measurements. However, error bars on these cross sections are large at low photon energies because of the very low absorbances measured; (these experiments were carried out primarily to get information at higher energies, where the cross sections are higher). Below 210 nm, therefore, our best cross sections are those obtained from the conventional and Fourier transform spectrometers. The Fourier transform experiments were carried out at relatively high resolution (~0.025 nm), and no fine structure was evident in the spectra (for clarity, not all points are shown in Fig. 1b). In Fig. 3, our preferred cross sections are compared on a logarithmic plot with the NASA recommendation values for atmospheric modeling, and the cross sections obtained by Rowland et al. [11]. The figure also shows the EEL data. Agreement between the data sets is mostly good, with biggest discrepancies in the region around 6.1 eV, where the cross section goes through a minimum. Here, the EEL values and those of Rowland et al. [11] are ~20% higher than the NASA recommendation, while the synchrotron cross sections are lower by 20%. The cross sections of Rowland et al. [11] extend to 190 nm (6.52 eV), where they are higher than the present values by ~30%; however, the two cross-section curves show the same general trend with increasing excitation energy. Cross sections are tabulated in Table 1; experimental DOSs over selected energy ranges are listed in Table 2.

4.2. Spectral assignments

It is helpful to discuss the electronic excitation spectrum of $ClONO_2$ in comparison with the spectra of simple aliphatic nitro-compounds, R–NO_2. In these, the electron density in a number of the frontier

Table 1c
Photoabsorption cross sections for chlorine nitrate derived from EEL measurement

λ/nm	Electron Energy/eV	Cross Section/Mb
247.8	5.00	0.91
238.5	5.20	1.26
229.4	5.40	1.99
221.4	5.60	2.91
213.6	5.80	3.42
206.7	6.00	3.36
199.8	6.20	3.79
193.7	6.40	5.14
187.7	6.60	7.72
182.3	6.80	10.72
177.0	7.00	14.00
172.2	7.20	16.67
167.4	7.40	19.08
163.1	7.60	21.71
158.8	7.80	25.10
154.9	8.00	27.14
151.2	8.20	27.58
147.6	8.40	24.51
144.2	8.60	22.71
140.8	8.80	25.79
137.8	9.00	34.20
134.7	9.20	52.84
131.9	9.40	53.18
129.1	9.60	41.21
126.5	9.80	38.25
123.9	10.00	30.04
121.6	10.20	26.82
119.2	10.40	27.30
117.0	10.60	30.49
114.7	10.80	34.23
112.7	11.00	37.55
110.6	11.20	37.61
108.7	11.40	43.63
106.8	11.60	44.00
105.1	11.80	41.97
103.3	12.00	42.52
101.6	12.20	44.00
99.9	12.40	45.39
98.4	12.60	46.75
96.8	12.80	50.56
95.3	13.00	54.91
93.9	13.20	54.70
92.5	13.40	55.63
91.2	13.60	56.42
89.8	13.80	58.54
88.6	14.00	60.98

molecular orbitals is concentrated at the NO_2 group. Electronic transitions involving these orbitals are, therefore, frequently discussed in the C_{2v} of the NO_2 group. The localized occupied MOs in these compounds are of type π (a_2 in C_{2v}, a″ in C_s), σ (a_1, a′), and σ (b_2, a′); of these, the b_2 (σ) orbital is generally described as n_O (oxygen nonbonding). There is also a low-lying unoccupied orbital, which is π^* (b_1, a″). In an early theoretical study of the electronic states of a series of nitro compounds, Harris [43] deduced that a typical spectrum will contain an intense transition to a state of type $\pi\pi^*$ around 6.5 eV, a low-intensity transition to a state $n_O\pi^*$ around 4.5 eV, and last, a weak transition to a state of type $\sigma\pi^*$ below 6.5 eV, whose excitation energy increases with increasing electronegativity of the substituent R group. These expectations are realized in the spectrum of, for example, nitromethane (CH_3NO_2), where the three types of transitions have been assigned to bands at (E_{max} values) 6.25, 4.25, and 4.5 eV, respectively [44].

A better comparison for $ClONO_2$ is with nitric acid $HONO_2$, from which chlorine nitrate is derived by replacement of H by Cl. The spectrum of nitric acid $HONO_2$ has a relatively strong band at 6.7 eV, assigned $\pi\pi^*$ [45]. This grows out of a weak absorption, $E_{max} \sim 4.6$ eV, which from its shape, contains at least two transitions expected to be of types $n_O\pi^*$ and $\sigma\pi^*$, respectively (see above). Theoretical studies support these conclusions. Thus, Bai and Segal [46] calculated vertical excitation energies (their descriptions) of 4.59 ($n\pi^*$), 5.59 ($n\pi^*$), and 6.88 eV ($\pi\pi^*$), respectively; more recently, Grana et al. [15] have obtained 4.78 ($n\pi^*$), 5.98 ($n\pi^*$), and 7.49 eV ($\pi\pi^*$). Although the two lower-lying states are denoted as $n\pi^*$, electron-density pictures provided by Grana et al. [15] show that while this is a good description of the lowest state, the electron-density redistribution associated with the middle one identifies it as the $\sigma\pi^*$ state of the NO_2 group. That is, for nitric acid, the long-wavelength end of the spectrum can be simply interpreted in terms of single-electron transitions between the NO_2-localized MOs [44] and associated computations [16,17].

The highest occupied molecular orbital (HOMO) of $ClONO_2$ (see above), orbital 5a″ ($IE = 11.56$ eV), is the $NO_2^{-}{}^{\pi}$ orbital, while orbital 18a′ ($IE = 12.94$ eV) is n_O [16]. It follows that, compared with $HONO_2$, the long-wavelength end of the $ClONO_2$

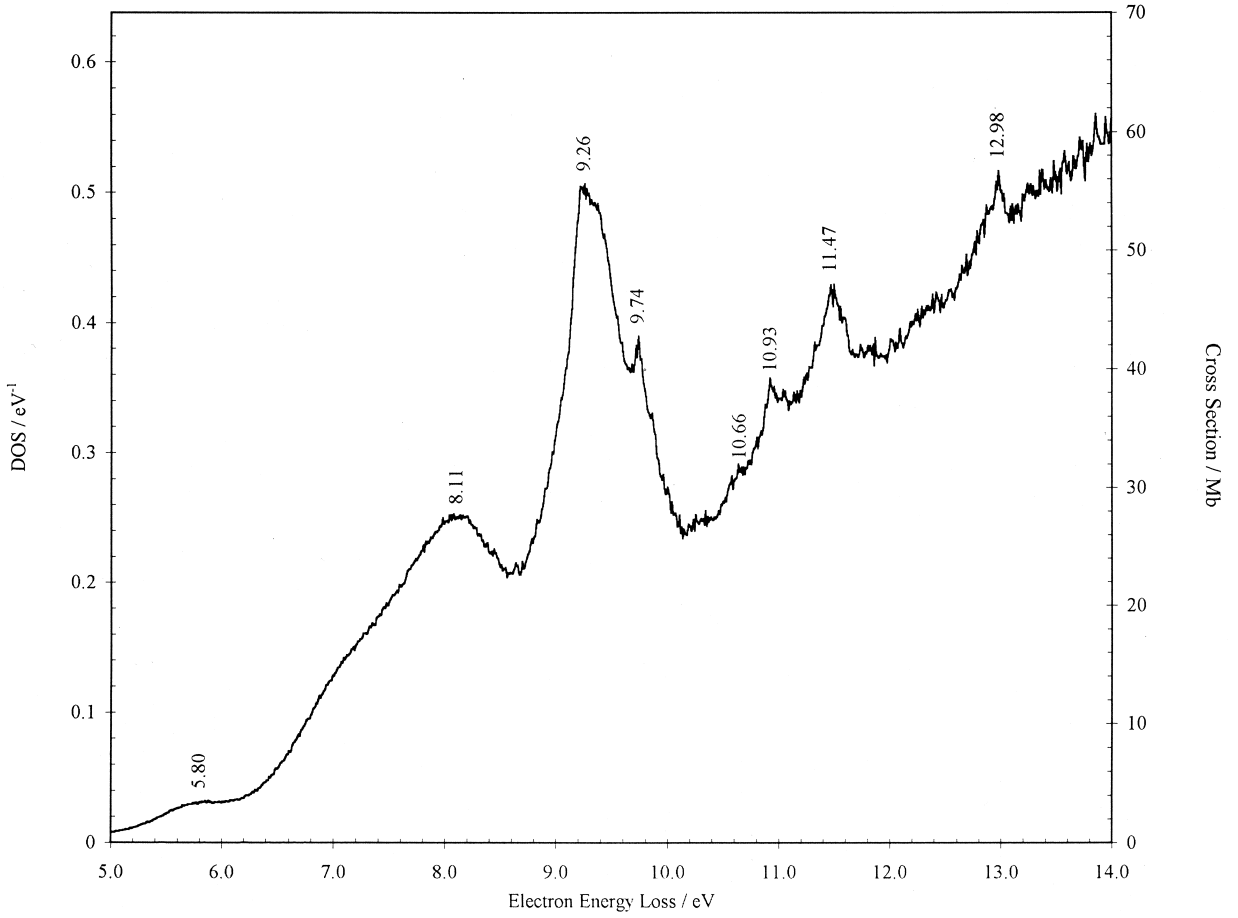

Fig. 2. Comparison of photoabsorption cross sections of chlorine nitrate recorded using synchrotron radiation and EEL spectroscopy. The previous data of Burkholder et al. [13] are also shown.

spectrum is expected to contain extra bands originating in orbitals 19a′ (n_{Cl}, IE = 12.14 eV) and 4a″ (π, IE = 12.94 eV). This is confirmed in the work of Grana et al. [15], who carried out a parallel theoretical study on the electronic states of $ClONO_2$ and $HONO_2$. We make use of their results in assigning the spectra (see Table 2 for a summary).

The first optical band is a low-intensity absorption at 3.2 eV. No excited singlet state is computed to lie around this energy. Further, the optical maximum is close to that observed in low-energy EEL (Fig. 4b) and that arises from a state whose excitation cross section is very high close to threshold. Accordingly, the first weak band is assigned to excitation of a triplet state. This fits with the computations in which the lowest excited triplet state ($^3n_O\sigma^*$, $^3A''$, where σ^* is Cl–O antibonding) is estimated at 3.4 eV [15]. This state has no equivalent in $HONO_2$. Computed energies for other low-lying triplet states are 4.3, 4.56, and 4.71 eV [15], all of which are within the first band of the near-threshold EEL spectra.

There is a very weak shoulder ~4.6 eV in the optical spectrum where one of the NO_2-group excitations, namely, $^1n_O\pi^*$ ($^1A_2$, $^1A''$, see above) is predicted. The calculated energy is 4.93 eV [15] (4.6 eV measured [11]). Another singlet state, $n_O\sigma^*$ $^1A''$ (which corresponds with the lowest-lying triplet) is computed at 4.36 eV [15]. As this has the higher calculated oscillator strength, we expect it also to contribute to the optical spectrum along with another

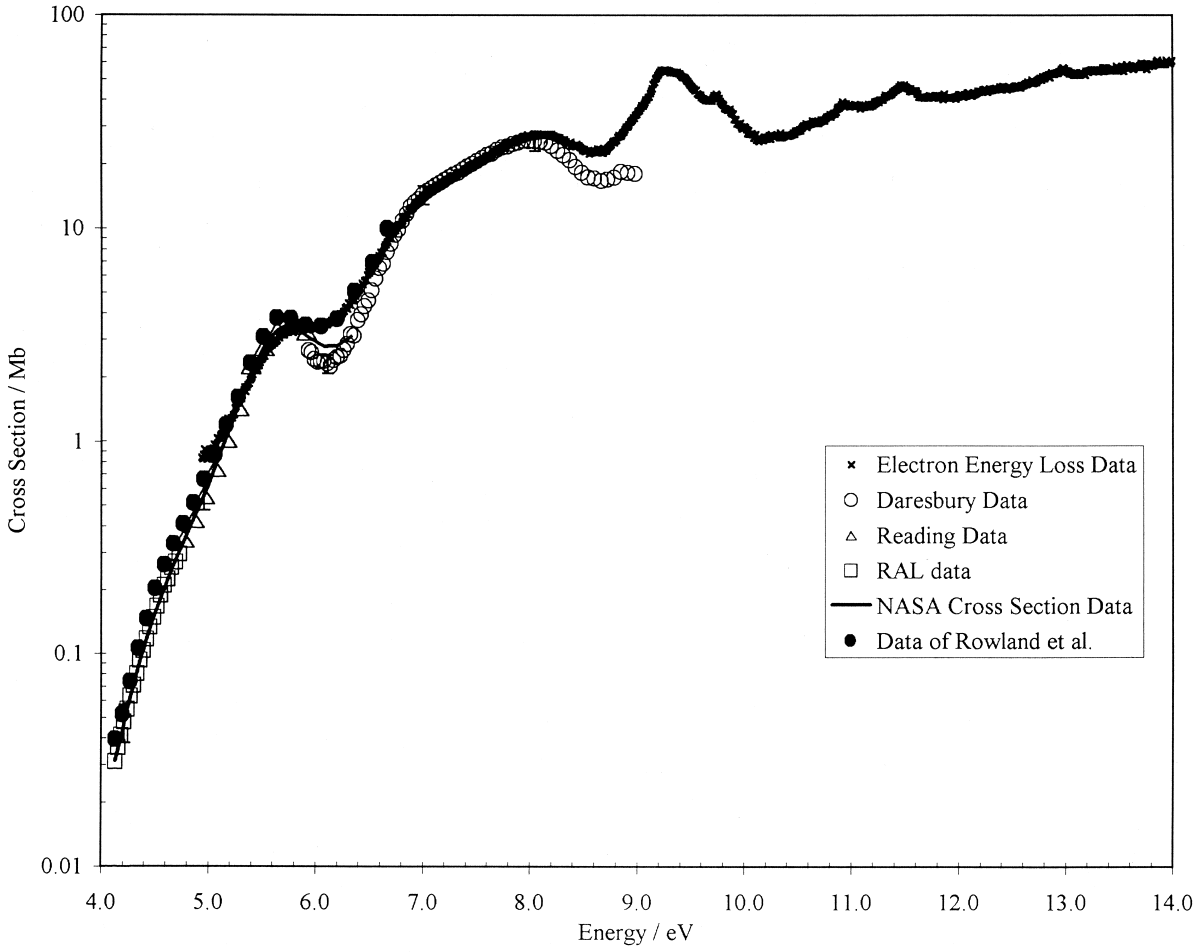

Fig. 3. (*a*) Total negative ion signal as a function of incident electron energy; (*b*) EEL spectrum recorded at a residual electron energy of ~0.5 eV. The signal arbitrary units are the same in each spectrum.

state of symmetry ^{1}A′ calculated to lie at 5.21 eV. The 5.77 eV maximum lies close to the energy computed for the $^1\sigma\pi^*$ (^{1}B$_1$, ^{1}A″) NO_2-group excitation (5.85 eV) and to that of a delocalized state of symmetry ^{1}A′ (6.47 eV) [15], both of which may contribute to the absorption band. The presence of more than one transition in this energy region is confirmed by the low-energy EEL data whose energy-loss maximum, 6 eV, is above the optical value. Of course, in the EEL case, spin-forbidden transitions may also contribute.

We then look for the $\pi\pi^*$ transition expected around 6.5 eV and detected at 6.7 eV in $HONO_2$ [45]. If the 5.8 eV absorption has been correctly identified, then the $\pi\pi^*$ transition lies within the broad composite band between 6 and 9 eV. Our assignment is to the 7.1 eV feature (6.62 eV computed [15]). The 8 eV peak has no equivalent structure in the spectrum of $HONO_2$. The shape and intensity point to an intravalence transition in which electron density is delocalized; its assignment must await further study. The 9.25 eV band has an analogue in $HONO_2$ (~9 eV, cross section ~30 Mb), as yet unassigned.

The lowest-lying Rydberg state of this molecule, resulting from promotion of an electron from the highest occupied (π, 5a″) orbital (*IE* ~ 11.56 eV) into a 3s orbital is expected around 8 eV. Also, in C_{2v} symmetry, the transition would be electric-dipole forbidden, and this will be reflected in a low intensity

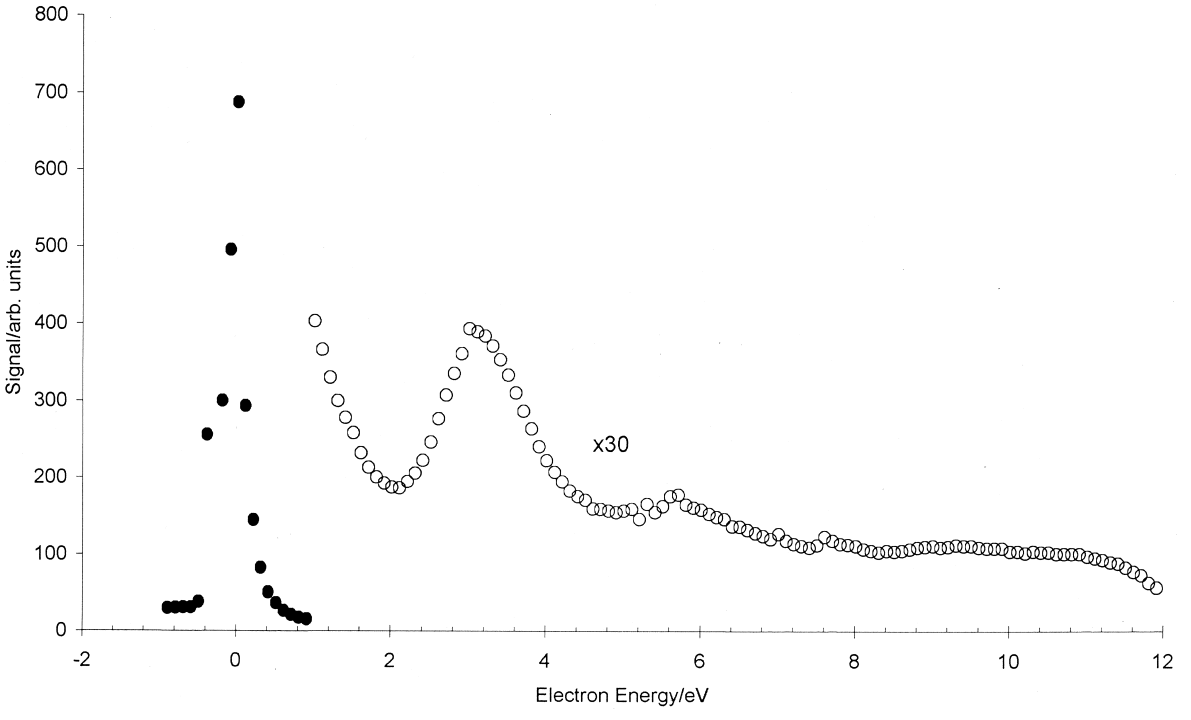

(a)

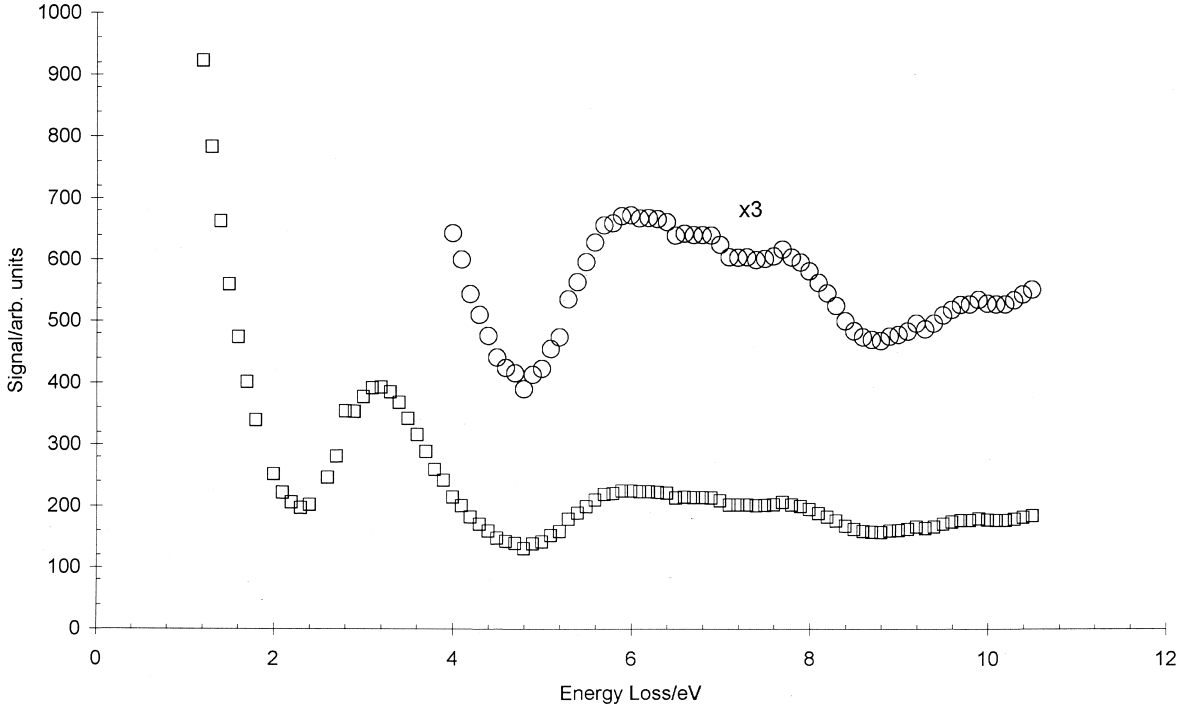

(b)

Fig. 4a,b. Photoelectron spectrum of chlorine nitrate. The region between 15.5 and 18 eV is contaminated with sharp features caused by molecular nitrogen.

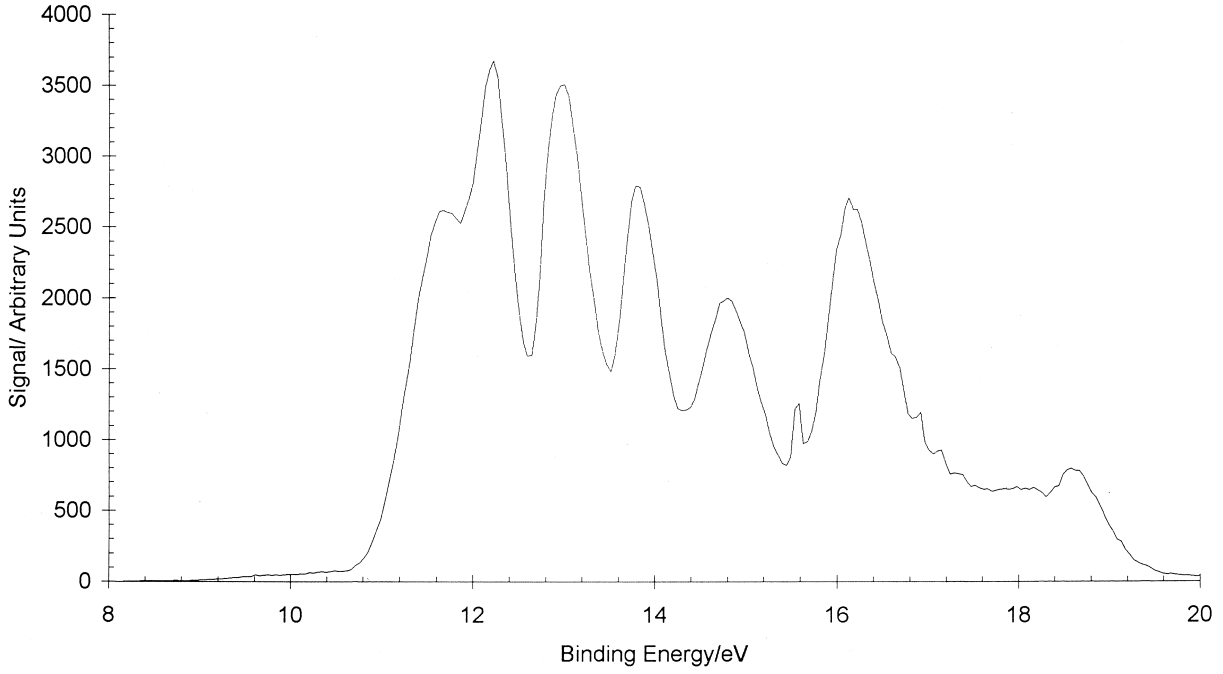

Fig. 5.

in the lower (C_s) point group. Consequently, it is probably obscured by the 8.1 eV peak. Excitations from the HOMO into the 3p Rydberg orbitals happen above the upper limit of the present optical spectrum and in the region of the feature around 9.3 eV in EEL. The weak features visible at high energy losses in the EEL spectrum of Fig. 2 may relate to excitation of Rydberg states.

Table 2
Differential oscillator strengths for chlorine nitrate

	Integrated Oscillator Strengths	
Energy Range/eV	EELS	Photoabsorption
4.13–6.17	0.033	0.028
6.17–8.64	0.399	0.372
8.64–9.67	0.377	
9.67–10.15	0.145	
10.15–10.45	0.075	
10.45–10.75	0.084	
10.75–11.13	0.124	
11.13–11.72	0.229	
11.72–12.57	0.336	
12.57–13.12	0.257	
13.12–14.24	0.587	

4.3. Dissociative electron attachment

The observation of a very large cross section for electron attachment close to zero electron energy is in accord with the results of a flow-drift tube experiment [18,19]. Future work on elucidation of the anionic

Table 3
Valence states in $ClONO_2$

Experiment				Theory [15]	
Optical		EEL			
Present Article	[11]	Fig. 2	Fig. 4b		State
	~3.2		3.2	3.43	$^3n_O\sigma^*$, $^3A''$
	~4.6			4.36	$^1n_O\sigma^*$, $^1A''$
				4.93	$^1n_O\pi^*$, $^1A''$
				5.21	$^1n_O\sigma^*$, $^1A'$
5.8		5.8		5.85	$^1\sigma\pi^*$, $^1A''$
			6.0	6.47	$^1A'$
~7.1		~7.1	6.8–7.1	6.62	$^1\pi\pi^*$, $^1A'$
				7.10	$^1A''$
				7.43	$^1A''$
			7.75–7.85		
8.0		8.1			

states and their dissociation dynamics should concentrate on electron energies of ~0, 3.0, and 5.75 eV, the last two peaks being located here for the first time.

5. Conclusions

In making the measurements described here, we have paid particular attention to sample purity. In no system did we detect any effects that could be ascribed to likely impurities or decomposition products such as Cl_2 and NO_2. Added to this, our UV and PES spectra are consistent with literature data. This is useful both as a test of sample purity and as a check of the previous data. We have extended the electronic spectrum using both optical and electron energy-loss methods and have offered spectral assignments guided by empirical rules for NO_2-containing compounds (which seem to apply here) and the results of published ab initio computations. However, it seems that there are optically allowed intravalence transitions that have yet to be characterized, and more theoretical effort is required for this. Finally, we have identified electron energies where dissociative electron attachment processes are important.

Acknowledgements

It is a pleasure to dedicate this article to Alex Stamatovic on the occasion of his sixtieth birthday. His pioneering work in the development of electron spectrometry has been an inspiration to all of us who have followed in this field. Two of us (N.C.J. and L.J.K.) acknowledge receipt of EPSRC postgraduate awards, and one of us (B.A.O.) a NERC postgraduate studentship. Funding for this project was provided by EPSRC, NERC (Laboratory Studies in Atmospheric Chemistry), and CLRC. The RAL Molecular Spectroscopy Facility thank NERC for support and R.G. Williams for technical assistance.

References

[1] S. Solomon, Rev. Geophys. 37 (1999) 275.
[2] J.C. Farman, B.G. Gardiner, J.D. Shanklin, Nature 315 (1985) 207.
[3] P.A. Newman, J.F. Gleason, R.D. McPeters, R.S. Stolarski, Geophys. Res. Lett. 24 (1997) 2689.
[4] J. Geophys. Res. 1989 94 special issues D9 and D14.
[5] Montreal Protocol on substances that may deplete the ozone layer. United Nations Environment Programme (UNEP), Nairobi, Kenya, 1987.
[6] S.A. Montzka, J.H. Butler, R.C. Myers, T.M. Thompson, T.H. Swanson, A.D. Clarke, L.T. Lock, J.W. Elkins, Science 272 (1996) 1318.
[7] D.M. Cunnold, R. Weiss, R.G. Prinn, D. Hartley, P.G. Simmonds, P.J. Fraser, B. Miller, F.N. Alyea, L. Porter, J. Geophys. Res. 102 (1997) 1259.
[8] M. Dameris, V. Grewe, R. Hein, C. Schnadt, Geophys. Res. Lett. 25 (1998) 3579.
[9] G. Marston, Ann. Rep. Pt. C 95 (1999) 235.
[10] W.B. DeMore, S.P. Sander, D.M. Golden, R.F. Hampson, M.J. Kurylo, C.J. Howard, A.R. Ravishankara, C.E. Kolb, M.J. Molina, JPL Publication 97-4 (1997) Evaluation 12.
[11] F.S. Rowland, J.E. Spencer, M.J. Molina, J. Phys. Chem. 80 (1976) 2711.
[12] L.T. Molina, M.J. Molina, J. Photochem. 11 (1979) 139.
[13] J.B. Burkholder, R.K. Talukdar, A.R. Ravishankara, Geophys. Res. Lett. 21 (1994) 585.
[14] S.L. Nikolaisen, S.P. Sander, R.R. Friedl, J. Phys. Chem. 100 (1996) 10165.
[15] A.J. Grana, T.J. Lee, M. Head-Gordon, J. Phys. Chem. 99 (1995) 3493.
[16] D. Wang, Y. Li, P. Jiang, X. Wang, B. Chen, Chem. Phys. Lett. 260 (1996) 99.
[17] C.G. Zhan, C.J. Zhang, Chem. Phys. Lett. 288 (1998) 15.
[18] J.M. Van Doren, A.A. Viggiano, R.A. Morris, T.M. Miller, J. Chem. Phys. 103 (1995) 10806.
[19] J.V. Seeley, T.M. Miller, A.A. Viggiano, J. Chem. Phys. 105 (1996) 2127.
[20] N.J. Mason, J.M. Gingell, J.A. Davis, H. Zhao, I.C. Walker, M.R.F. Siggel, J. Phys. B 29 (1996) 3075.
[21] F. Motte-Tollet, M.P. Ska, G. Marston, I.C. Walker, M.R.F. Siggel, J.M. Gingell, L. Kaminski, K.L. Brown, N.J. Mason, Chem. Phys. Lett. 282 (1997) 275.
[22] G. Marston, I.C. Walker, N.J. Mason, J.M. Gingell, H. Zhao, K.L. Brown, F. Motte-Tollet, J. Delwiche, M.R.F. Siggel, J. Phys. B 31 (1998) 3387.
[23] N. Mohammed-Tahrin, A.M. South, D.A. Newnham, R.L. Jones, J. Geophys. Res. (submitted, 2000).
[24] M. Schmeiser, Inorg. Syn. 9 (1967) 127.
[25] J.M. Gingell, N.J. Mason, H. Zhao, I.C. Walker, M.R.F. Siggel, J. Phys. B 32 (1999) 5229.
[26] M. Inoeuki, Rev. Mod. Phys. 43 (1971) 297.
[27] R.H. Huebner, R.J. Celotta, S.R. Mielczarek, C.E. Kuyatt, J. Chem. Phys. 59 (1973) 5434.
[28] J.W. Gallagher, C.E. Brion, J.A.R. Samson, P.W. Langhoff, J. Phys. Ref. Data 17 (1988) 9.
[29] W.F. Chan, G. Cooper, C.E. Brion, Chem. Phys. Lett. 170 (1993) 111.
[30] C.E. Kuyatt, 1968 in B. Bederson and W. Fite, eds. Methods in Experimental Physics, Vol. 7 Pt. A1.

[31] R.H. Huebner, R.J. Celotta, S.R. Mielczarek, C.E. Kuyatt, J. Chem. Phys. 63 (1975) 241.
[32] R.H. Huebner, S.R. Mielczarek, C.E. Kuyatt, Chem. Phys. Lett. 16 (1972) 464.
[33] T. Ari, H. Guven, N. Ecevit, J. Electr. Spectrosc. Rel. Phenom. 73 (1995) 13.
[34] W.M. Johnstone, N.J. Mason, W.R. Newell, P. Biggs, G. Marston, R.P. Wayne, J. Phys. B 25 (1992) 3873.
[35] J.A. Davies, N.J. Mason, G. Marston, R.P. Wayne, J. Phys. B 28 (1995) 4179.
[36] J.M. Gingell, N.J. Mason, H. Zhao, I.C. Walker, M.R.F. Siggel, Chem. Phys. 220 (1997) 191.
[37] J.M. Gingell, G. Marston, N.J. Mason, H. Zhao, M.R.F. Siggel, Chem. Phys. 237 (1998) 443.
[38] J.A. Davies, PhD thesis University of London (1995).
[39] I.C. Walker, J.M. Gingell, J.A. Davies, N.J. Mason, 2000 in preparation.
[40] G.A. Keenan, I.C. Walker, D.F. Dance, J. Phys. B 15 (1982) 2509.
[41] A. Stamatovic, G.J. Schulz, Rev. Sci. Instr. 41 (1970) 423.
[42] M. Cheetham, Internal Daresbury Report (1999).
[43] L.E. Harris, J. Chem. Phys. 58 (1973) 5615.
[44] I.C. Walker, M.A.D. Fluendy, Int. J. Mass Spectrom. 202 (2000).
[45] M. Suto, L.C. Lee, J. Chem. Phys. 81 (1984) 1294.
[46] Y.Y. Bai, G.A. Segal, J. Chem. Phys. 92 (1990) 7429.